

A zero dimensional study of Ohmically heated negative triangularity tokamaks

A. Balestri¹, J. Ball¹, and S. Coda¹
¹*École Polytechnique Fédérale de Lausanne (EPFL),
Swiss Plasma Center (SPC), 1015 Lausanne, Switzerland*

Because negative triangularity plasma scenarios remain in L-mode, they do not require external heating systems that exceed the H-mode power threshold. Operating with less heating has the potential to improve performance as heating generally degrades confinement in tokamaks. Using simple zero dimensional power balance and standard empirical scaling laws for confinement, we analyze the impact of external heating on several different reactor-relevant devices (i.e. SPARC, MANTA, ITER and DEMO). We compare the nominal externally heated scenarios against equivalent negative triangularity cases without external heating. For most of these devices, the Ohmically heated negative triangularity versions achieve better performance, particularly for devices with high magnetic field and/or high fusion gain.

Keywords: fusion plasma, negative triangularity, Ohmic heating, fusion power plant, ignition

Introduction The vast majority of designs for reactor-relevant tokamaks (e.g. ITER, DEMO, SPARC) employ Positive Triangularity (PT) plasma shaping and powerful heating systems to generate large quantities of fusion power. Powerful heating systems are required as these designs typically rely on H-mode (High confinement mode) plasma scenarios. In H-mode, an edge transport barrier forms (i.e. the pedestal), which is defined by strong gradients of pressure. This, in turn, increases the pressure reached in the core of the plasma and is reflected in a higher global energy confinement time. Crucially, sustaining an H-mode scenario requires one to exceed a heating power threshold, which can be tens of megawatts [1, 2]. This drives the need for complex and expensive heating systems that require a lot of external electricity. For these reasons, reactor designs typically operate with the minimal amount of heating needed to trigger H-mode [3].

While H-mode achieves excellent energy confinement, it has a serious drawback. The pedestal is not stable, but undergoes periodic relaxations called Edge Localized Modes (ELMs). In future power plants, ELMs are expected to unleash huge fluxes of energy and particles against plasma facing components of a reactor, exceeding material survivability limits. This has deepened interest in an attractive alternative: Negative Triangularity (NT). While PT plasmas have a poloidal cross-section shaped like a “D” (with the axis of symmetry on the left), NT plasmas are shaped like a “C”. In the last two decades, experiments [4–10] and simulations [11–16] have progressively revealed several advantages of NT. First, NT plasmas are *not* able to sustain a strong edge transport barrier [17], even at high heating power. Instead they remain in L-mode (Low confinement mode), the most robust ELM-free scenario. Second, NT displays a reduction of turbulent transport, which allows a NT plasma to sustain strong plasma gradients in the outer-core and obtain central core pressures similar to a standard PT H-mode. Thus, NT looks to achieve H-mode-

like global confinement, while remaining in L-mode and avoiding ELMs. Additionally, this means that the constraint of exceeding the L-H power threshold vanishes and auxiliary heating systems are no longer required to improve confinement. In this paper, we will consider the question “What is the ideal amount of heating power for a NT tokamak?” In particular we will consider NT plasmas with the minimum amount of heating possible: only the Ohmic heating that arises from the plasma current.

Methodology To assess the performance of an Ohmic NT scenario, we use a simple zero-dimensional (0D) power balance approach. A simple form of the power balance equation can be written as

$$\left\langle \frac{dW}{dt} \right\rangle = \langle P_\alpha \rangle + \langle P_\Omega \rangle + \langle P_{ext} \rangle - \langle P_{rad} \rangle - \langle P_{loss} \rangle, \quad (1)$$

where dW/dt is the time variation of thermal energy density stored in the plasma, P_α is the power density released by the α particles produced by fusion reactions, P_Ω is the Ohmic heating power density generated by the electric current flowing in the plasma, P_{ext} is the external heating power density injected by external systems (e.g. neutral beam injection, radiofrequency heating), P_{rad} is the power density radiated by the plasma and P_{loss} is the power density lost through convection (primarily turbulent transport). The $\langle \dots \rangle$ operator is a volume average over the entire plasma, which allows us to consider profile effects. This operation requires knowledge of how temperature (T) and density (n) vary with radius, which is set by transport processes that are beyond the simple analysis in this work. Hence, we will use simple analytical profiles which allows to write the volume averaged quantities as

$$\langle f \rangle = \frac{\int dV f(r)}{\int dV} = \frac{f_0}{1 + \alpha_f}, \quad (2)$$

where the integral is performed over the plasma volume. Here f is a placeholder for T and n , and α_f is what we refer to as *peaking factor*. For the following analysis,

the peaking factors of temperature and density will be free parameters, as their values can only be determined by solving the full transport equations. Moreover, to keep the analysis as simple as possible, we assume that electron and ion densities and temperatures are the same.

The equilibrium state is set by $dW/dt = 0$, i.e. when the sources are balanced by the sinks in the power balance equation. We will consider density to be a free parameter, as it can be fixed by changing the fueling. Thus, the condition $dW/dt = 0$ sets the temperature(s) that can be achieved by the plasma in steady-state. However, another important concept is the stability of this equilibrium state, which is set by the variation of dW/dt with temperature. When $\frac{\partial}{\partial T}(\frac{dW}{dt}) \geq 0$, the plasma state is unstable, while $\frac{\partial}{\partial T}(\frac{dW}{dt}) \leq 0$ corresponds to a stable state. In this work, we will use power balance to determine the steady-state temperatures and compute

the associated fusion power $P_{fus} = 5P_\alpha$ and fusion gain $Q = P_{fus}/(P_\Omega + P_{ext})$.

We now make explicit all the terms on the right hand side of equation (1). The α power density is given by [18]

$$\langle P_\alpha \rangle = \left\langle \frac{E_\alpha}{4} n^2 C_0 \zeta^{-5/6} \xi^2 e^{-3\zeta^{1/3}\xi} \right\rangle, \quad (3)$$

where $E_\alpha = 3500 \text{ keV}$ is the energy of the α particles produced by deuterium-tritium fusion reactions, $C_0 = 6.4341 \times 10^{-20}$, $\xi = C_1/(T^{1/3})$, $\zeta = 1 - (C_2T + C_4T^2 + C_6T^6)/(1 + C_3T + C_5T^2 + C_7T^3)$, $C_1 = 6.661 \text{ keV}^{1/3}$, $C_2 = 1.5136 \times 10^{-2} \text{ keV}^{-1}$, $C_3 = 7.5189 \times 10^{-2} \text{ keV}^{-1}$, $C_4 = 4.6064 \times 10^{-3} \text{ keV}^{-2}$, $C_5 = 1.35 \times 10^{-2} \text{ keV}^{-2}$, $C_6 = -1.0675 \times 10^{-4} \text{ keV}^{-3}$, $C_7 = 1.366 \times 10^{-5} \text{ keV}^{-3}$. The Ohmic power density is

$$\langle P_\Omega \rangle = \langle \eta j^2 \rangle = \frac{\eta_S}{(1 - \epsilon^{1/2})^2 T_0^{3/2}} \left(\frac{I_p}{a^2 \mathcal{F}(\kappa_{95}, \delta_{95}, \epsilon)} \right)^2 \frac{(1 + \kappa_0^2)^2 (1 + \alpha_T)^2}{27\kappa_0^2 (1 + 0.5\alpha_T)}, \quad (4)$$

where η is the resistivity, j is the current density profile, $\eta_S = 1.64 \times 10^8 Z_{eff} m s^{-1} A^{-2} \text{ keV}^{2.5}$ is the Spitzer resistivity coefficient, Z_{eff} is the plasma effective charge, $\epsilon = a/R$ is the inverse aspect ratio, I_p is the plasma current in A, $\mathcal{F}(\kappa_{95}, \delta_{95}, \epsilon) = 4.1 \times 10^6 (1 + 1.2(\kappa_{95} - 1) + 0.56(\kappa_{95} - 1)^2)(1 + 0.09\delta_{95} + 0.16\delta_{95}^2) \frac{1+0.45\delta_{95}\epsilon}{1-0.74\epsilon}$ is a function that depends only on geometry and is used to correctly express the current density in terms of I_p [19], κ_0 is the elongation on axis, and κ_{95} and δ_{95} are the elongation and triangularity at the flux surface enclosing 95% of the poloidal flux. The radiated power density is

$$\langle P_{rad} \rangle = C_B Z_{eff} \frac{n_0^2 T_0^{1/2}}{1 + 2\alpha_n + 0.5\alpha_T}, \quad (5)$$

where $C_B = 3.3 \times 10^{-21} \text{ m}^3 \text{ sec}^{-1} \text{ keV}^{-2.5}$. Here, we are considering only Bremsstrahlung radiation, as it is typically the dominant contribution to the power lost by radiation. The power density lost due through convection is extraordinarily difficult to predict from first-principles as it is dominated by turbulence. For that reason, we will use empirical scaling laws based on experimental results for the energy confinement time τ_E [20]. This enables us to write the loss term as

$$\langle P_{loss} \rangle = \frac{3n_0 T_0}{\tau_E (1 + \alpha_n + \alpha_T)}, \quad (6)$$

where the factor 3 comes from the assumption that electrons and ions have the same temperature and density. Finally, the external power density is assumed to be constant, regardless of the plasma properties.

The only quantities that we have not yet specified in equation (1) are τ_E , α_T and α_n . For α_T and α_n we will use typical values from theory or experiments. For τ_E we use the most widely accepted scaling laws with one caveat. As Ohmic heating is a key aspect of this work, we cannot simply use scaling laws based primarily on externally heated plasmas. Indeed, as showed in many publications [21], confinement in Ohmic plasmas has unique behavior. It scales linearly with density in the so-called Linear Ohmic Confinement regime and transitions to an externally heated scaling law once a critical density is reached (i.e. the LOC-SOC transition). However, we also cannot exclusively use Ohmic scaling laws because the α heating becomes significant at high performance. This represents ‘‘external’’ heating (as it is a distinct source of heating absent from all past experimental Ohmic discharges). For these reasons we employ the method developed in Ref. [22] to unify Ohmic and externally heated energy confinement scaling laws. This takes the form

$$\tau_E = \tau_\Omega \left(\frac{P_\Omega}{P} \right) + \tau_{heat} \left(1 - \frac{P_\Omega}{P} \right), \quad (7)$$

where τ_Ω is the confinement time relative to the Linear Ohmic Confinement scaling and τ_{heat} is the scaling for the heated part. The terms P_Ω/P and $1 - P_\Omega/P$ are used to weight the two confinement times according to the relative sizes of the Ohmic and total heating $P = P_\alpha + P_\Omega + P_{ext}$.

For the Ohmic part of the confinement scaling, we use

the standard Neo-Alcator scaling law [20]

$$\tau_{\Omega} = 0.007 H_{NA} \langle n_{19} \rangle \kappa_{95} a R^2 q_{95}, \quad (8)$$

where H_{NA} is a confinement enhancement factor and q_{95} is the value of the safety factor at the flux surface enclosing 95% of the poloidal flux. H_{NA} is set to 1 for the best prediction of standard performance, but it can also be used to adjust for considerations not included in the scaling (e.g. NT geometry). For the heated part of the scaling we use either the ITER-98y2 H-mode scaling [23]

$$\tau_E^{98} = 0.0562 H_{98} I_p^{0.93} B^{0.15} n_{19}^{0.41} M^{0.19} R^{1.39} a^{0.58} \kappa_a^{0.78} P^{-0.69} \quad (9)$$

or the ITER-89P L-mode scaling [24]

$$\tau_E^{89} = 0.048 H_{89} I_p^{0.85} B^{0.2} n_{20}^{0.1} M^{0.5} R^{1.2} a^{0.3} \kappa_a^{0.5} P^{-0.5}, \quad (10)$$

where I_p is the plasma current in MA , n_{19} and n_{20} are the plasma number density in $10^{19}m^{-3}$ and $10^{20}m^{-3}$ respectively, B is the magnetic field in T , M is the average ion mass in amu , R and a are the major and minor radius in m , κ_a is the elongation at the Last Closed Flux Surface (LCFS), and P is the total heating power in MW . Importantly, P includes all heating powers, i.e. P_{α} , P_{Ω} and possibly P_{ext} . It is important to note that the negative exponent in the heating power factor of the two scaling laws means that weak external heating enables higher confinement time. Like H_{NA} , the confinement enhancement factors H_{98} and H_{89} are scalar quantities that represent how much better or worse is confinement with respect to the nominal scaling law (e.g. $H_{98} = 1$ or $H_{89} = 1$). These three confinement factors represent the biggest uncertainty in predicting how a NT plasma will behave. Since no existing scaling law incorporates NT, one is forced to account for NT by choosing representative confinement enhancement factors. A large number of NT discharges produced on TCV (figure 1(a)) and DIII-D [17, 25] indicate that the H-mode scaling of equation (9) with $H_{98} = 1$ is a good fit for the experimental performance of heated NT plasmas. However, we will also consider a range of possible confinement quality by using the ITER-89P scaling with different values of H_{89} . Regarding, the enhancement factor for the Neo-Alcator scaling law, a preliminary analysis of the TCV NT database suggest that a factor of $H_{NA} = 2$ can be easily achieved (figure 1(b)) and it is our choice for the following analysis.

Results Using equation (1), we can estimate the operating point of various tokamak designs to understanding the impact of external heating on NT plasmas, as well as compare NT with existing PT H-mode designs. We will consider four reactor-relevant tokamaks: MANTA [26], SPARC [3], ITER [27] and DEMO [28]. Table I shows their parameters.

These machines were chosen because they represent different parts of parameter space. SPARC is relatively small with a very large magnetic field, MANTA

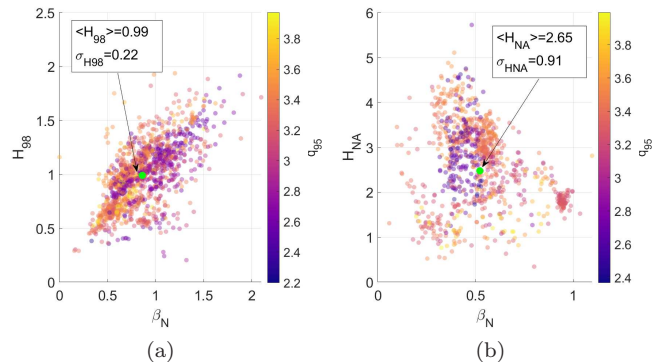


FIG. 1. (a) ITER98 and (b) Neo-Alcator confinement enhancement factors as functions of normalized β and q_{95} from stationary NT TCV shots. The green dots represent the centroids of the clusters of experimental data.

	MANTA	SPARC	ITER	DEMO
$I_p [MA]$	10	8.7	15	19.6
$B_T [T]$	11	12.2	5.3	5.7
$a [m]$	1.2	0.57	2.0	3.0
$R [m]$	4.55	1.85	6.2	9.1
κ_{95}	1.4	1.7	1.6	1.6
δ_{95}	-0.5	0.45	0.33	0.33
Z_{eff}	1.5	1.5	1.5	1.5
α_T	1.5	1.5	0.5	1.5
α_n	0.3	0.33	0.2	0.3
P_{ext}	40	11	40	50
Q^{target}	15	11	10	40

TABLE I. Main parameters for the considered tokamaks.

is medium-sized with a large magnetic field, ITER is large with relatively low magnetic field and DEMO is very large with low magnetic field. MANTA is designed for NT, while all the others use PT. Note that the density peaking factors for SPARC, ITER and DEMO are all for H-mode plasmas. However, it is expected that NT L-mode plasmas will have higher density peaking, as they lack an H-mode pedestal. Regardless, we will use standard H-mode peaking factors for all cases, which will tend to underpredict the performance of NT L-mode.

We start by comparing NT MANTA scenarios with different energy confinement time scaling laws and enhancement factors. In figure 2 we show operating space plots for the Ohmic scenario (a,d) and scenarios with different levels of external heating (b,c,e,f). In the first row, we assume that NT can achieve H-mode-like performance $H_{98y2} = 1$ for the auxiliary heated global confinement time. In the second row, we are more conservative and take L-mode confinement with a small enhancement factor $H_{89} = 1.4$. In both rows, we take $H_{NA} = 2.0$ for the Ohmic part of the confinement time scaling. These plots show dW/dt over a temperature-density space. The conditions that the device would actually achieve in steady state are represented by the $dW/dt = 0$ line, i.e. where

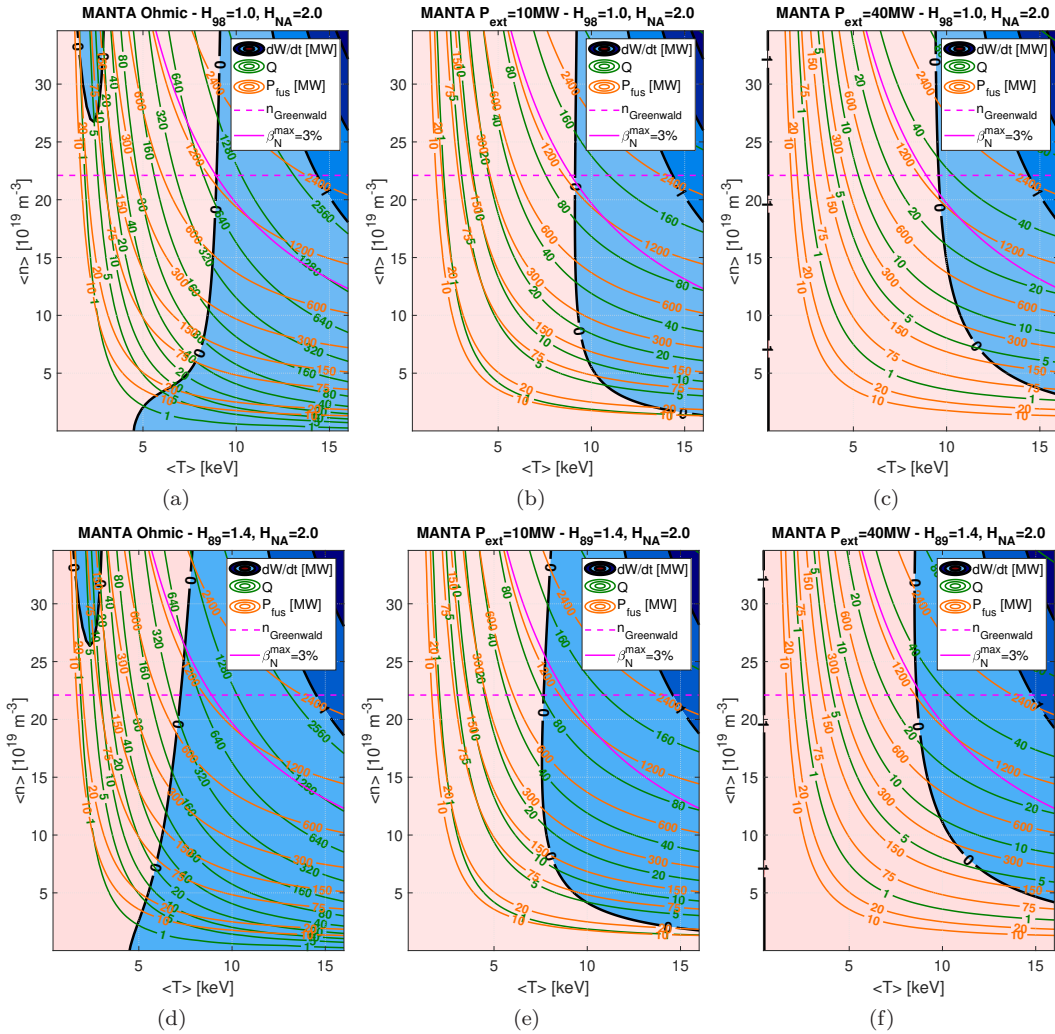


FIG. 2. Contour plots of the dW/dt function in temperature-density space for MANTA scenarios with different external heating power and confinement time scalings. The green lines indicate constant fusion gain Q , the yellow lines indicate constant fusion power P_{fus} , the dashed magenta line indicates the Greenwald density limit and the solid magenta line the Troyon β_N limit.

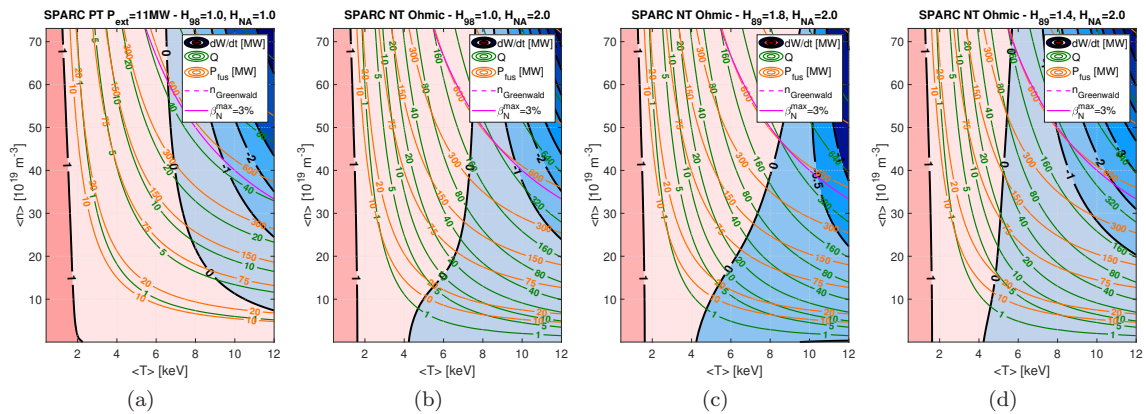


FIG. 3. Contour plots of the dW/dt function in temperature-density space for different SPARC PT (a) and NT (b,c,d) scenarios with H-mode or enhanced L-mode confinement time scalings. The various contour lines have the same meaning as in figure 2.

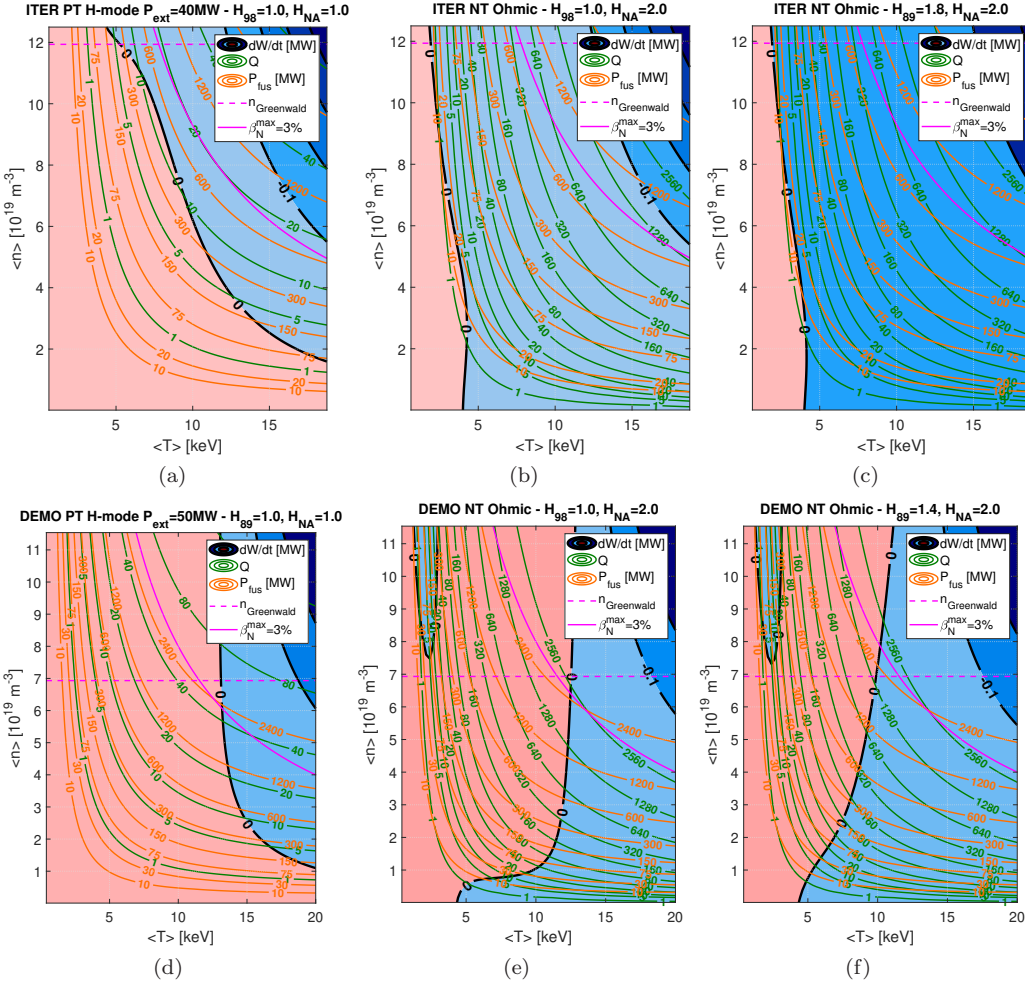


FIG. 4. Contour plots of the dW/dt function in temperature-density space for different ITER PT (a) and NT (b,c) scenarios with H-mode or enhanced L-mode confinement time scaling, and for DEMO PT (d) and NT (e,f) scenarios with H-mode or enhanced L-mode confinement time scaling. The various contour lines have the same meaning as in figure 2.

the color goes from red to light blue. As the density can be considered to be a free parameter (set by the fueling systems), the $dW/dt = 0$ line shows the achievable values of temperature. On the same plots, we also display contours of fusion gain Q and total fusion power ($P_{fus} = 5P_{\alpha}$) as well as the Greenwald density limit [29] and the Troyon β limit [30] (i.e. $\beta_N \simeq 3\%$). These limits bound the region where safe operations can be more easily achieved.

The first row of figure 2 shows that, in case of H-mode-like confinement, the Ohmic scenario is preferable over the heated cases because the same fusion power can be reached at much larger fusion gain, which correspond to higher effective electrical power produced by the reactor. For instance, if we compare figure 2(a) and 2(c), we observe that, just below the Greenwald limit, both the Ohmic and heated cases reach the same fusion power $P_{fus} \simeq 1.2 GW$. However, the Ohmic scenario has a fusion gain of $Q \simeq 640$, while the case heated with ex-

ternal power of $P_{ext} = 40 MW$ has $Q \simeq 30$. We explain these observations by noticing that, at the chosen operation point, the external heating is negligible compared to the α heating. The only place where the P_{ext} cannot be neglected is the denominator of the fusion gain Q (as here it is not summed with P_{α}). While we have argued that H-mode-like confinement is the most appropriate for NT plasmas, we can also study the effect of a more pessimistic confinement scaling. To do so, we use the L-mode scaling with an enhancement factor of $H_{89} = 1.4$, which appears a very conservative prediction for the confinement of reactor-relevant NT plasmas. In the second row of figure 2, we observe that the Ohmic scenario achieves the same range of total fusion power as the heated case with $P_{ext} = 10 MW$, but slightly less fusion power than the case with $P_{ext} = 40 MW$. However, the Ohmic scenario is still able to reach much larger fusion gain Q .

For MANTA, we conclude that external heating is

not necessary and is in fact detrimental. This is because MANTA has a high magnetic field and is sufficiently large to reach good performance. Ohmic heating alone should allow it to access regions of the density-temperature space where large quantities of P_α are produced. Adding external power that represents a small fraction of P_{fus} only lowers the fusion gain. Moreover, by increasing the recirculating power it also reduces the amount of net electricity produced.

Next we will compare a PT H-mode scenario against a NT Ohmically heated one. Specifically, we will consider the PT H-mode scenario envisioned for the SPARC tokamak (which includes $P_{ext} = 11 MW$ of ICRF heating) against an artificial Ohmically heated NT scenario. To produce the NT scenario, we will simply flip the triangularity of the PT SPARC scenario. This affects equation (1) only in that we use different scaling laws for energy confinement time (i.e. equation (7) instead of equation (9)). The results are shown in figure 3. At the nominal volume averaged density of $\langle n \rangle = 31 \times 10^{19} m^{-3}$ planned for SPARC, the PT H-mode scenario achieves a volume averaged temperature of $\langle T \rangle = 7.5$ keV, a fusion power of $P_{fus} = 150 MW$ and a fusion gain of $Q = 15$. As a benchmark of our model, we note that these values agree well with the nominal operation point found in [3], predicted by means of much more rigorous calculations. If we assume the H-mode scaling is valid for NT, the same fusion power of PT H-mode can be reached in an Ohmically heated NT plasma and at a much higher fusion gain of $Q = 80$. Even if an L-mode scaling is used for NT, the picture does not change much. With an L-mode enhancement factor of $H_{89} = 1.8$, the fusion power and fusion gain remain the same as for H-mode-like confinement. Even with a more pessimistic factor of $H_{89} = 1.4$, the same fusion power can still be reached, albeit requiring a slightly higher density. Given that flipping the triangularity of SPARC may force one to reduce the magnetic field (due to increased mechanical forces in the coil), we note that the same performance of the PT H-mode SPARC scenario can be achieved by an NT Ohmic H-mode-like case with $B_T = 9.5 T$ (holding I_p constant). In fact, it is possible to achieve the same performance at even lower magnetic field (again holding I_p constant), but this would lower q_{95} below the critical threshold for the external kink limit (i.e. $q_{95} \simeq 2$). Lastly, we remind the reader that the confinement benefits of lower heating power are not restricted to NT plasmas. For example, the SPARC PT *L-mode* scenario [3] employs 24.1 MW of external ICRF heating and produces 55 MW of fusion power, leading to a fusion gain of $Q = 2.2$. However, we observe that the same fusion gain can be reached in Ohmic conditions at larger density ($\langle n \rangle \simeq 2.6 \times 10^{20} m^{-3}$), lower temperature ($\langle T \rangle \simeq 3$ keV) and lower fusion power ($P_{fus} = 10 MW$). Interestingly, the fact that the fusion power is lower might be attractive if one wants to demonstrate breakeven while minimizing the neutron activation

of the machine.

Up to now, we have considered machines with large magnetic fields ($B_T \geq 10 T$), which is known to be beneficial for Ohmic heating. Let us now consider ITER and DEMO, which are large machines with relatively weaker on-axis magnetic field ($B_T \simeq 5 T$). In figure 4(a) we show the comparison between the reference ITER PT H-mode scenario (which includes 40 MW of external heating) and two artificial NT cases: one with H-mode-like confinement (figure 4(b)) and the other with enhanced L-mode confinement (figure 4(c)). In figure 4(d) we show the comparison between the reference DEMO PT H-mode scenario (which includes 50 MW of external heating) and two artificial NT cases: one with H-mode-like confinement (figure 4(b)) and the other with enhanced L-mode confinement (figure 4(c)). We note that our analysis reproduces the expected performance of the nominal ITER and DEMO PT H-mode scenarios well. In evaluating the Ohmic NT scenario, we see an important impact due to the size difference between the two devices. DEMO is bigger than ITER, which enables it to reach larger Q . For ITER, we see that neither of the NT scenarios are able to reach the same performance of the PT case. This is because the Ohmic power is too weak and the confinement too poor in the NT Ohmic cases to heat the plasma past $\langle T \rangle = 5$ keV. This temperature is important as it is roughly the temperature at which the fusion cross-section starts to be substantial. On the other hand, we see that the Ohmic NT scenario is preferable in DEMO (as it reaches a similar fusion power as the heated PT case and at a much higher fusion gain). Since DEMO is bigger than ITER, it has a longer energy confinement time, enabling the Ohmic power to heat the plasma past 5 keV (beyond which α heating takes over).

Conclusions In this work, we used 0D power balance to analyze the amount of heating power needed for a NT tokamak to produce fusion power and achieve large fusion gain. In this framework, we focused on NT plasmas with Ohmic heating only, which is the lowest possible amount of heating (as it is necessarily generated by the plasma current). While reducing the heating power did not enable more fusion power, it can allow a machine to achieve higher fusion gain Q and minimize recirculating power. We made several comparisons with four machines characterized by different size, magnetic field and fusion gain: MANTA, SPARC, ITER and DEMO. We observed that NT ohmic operations are an attractive option for MANTA, SPARC and DEMO, while they are detrimental for ITER. These comparisons indicated that an Ohmic NT scenario is most attractive for design points with high fusion gain ($Q \gtrsim 10$), especially when achieved using a strong magnetic field (as opposed to large size).

Acknowledgments This work has been carried out within the framework of the EUROfusion Consortium, via the Euratom Research and Training Programme (Grant Agreement No 101052200 - EUROfusion) and

funded by the Swiss State Secretariat for Education, Research and Innovation (SERI). Views and opinions expressed are however those of the author(s) only and do not necessarily reflect those of the European Union, the European Commission, or SERI. Neither the European Union nor the European Commission nor SERI can be held responsible for them. This work was supported in part by the Swiss National Science Foundation.

-
- [1] Y. R. Martin, T. Takizuka, and (and the ITPA CDBM H-mode Threshold Database Working Group), Power requirement for accessing the h-mode in iter, *Journal of Physics: Conference Series* **123**, 012033 (2008).
- [2] R. Behn, B. Labit, B. P. Duval, A. Karpushov, Y. Martin, L. Porte, and T. Team, Threshold power for the transition into h-mode for h, d, and he plasmas in tcv, *Plasma Physics and Controlled Fusion* **57**, 025007 (2014).
- [3] A. J. Creely, M. J. Greenwald, S. B. Ballinger, D. Brunner, J. Canik, J. Doody, T. Fülöp, D. T. Garnier, R. Granetz, T. K. Gray, and et al., Overview of the sparc tokamak, *Journal of Plasma Physics* **86**, 865860502 (2020).
- [4] Y. Camenen, A. Pochelon, R. Behn, A. Bottino, A. Bortolon, S. Coda, A. Karpushov, O. Sauter, G. Zhuang, and the TCV team, Impact of plasma triangularity and collisionality on electron heat transport in TCV L-mode plasmas, *Nuclear Fusion* **47**, 510 (2007).
- [5] M. Fontana, L. Porte, S. Coda, and O. S. and, The effect of triangularity on fluctuations in a tokamak plasma, *Nuclear Fusion* **58**, 024002 (2017).
- [6] S. Coda, A. Merle, O. Sauter, L. Porte, F. Bagnato, J. Boedo, T. Bolzonella, O. Février, B. Labit, A. Marinoni, A. Pau, L. Pigatto, U. Sheikh, C. Tsui, M. Vallar, T. Vu, and T. T. Team, Enhanced confinement in diverted negative-triangularity L-mode plasmas in TCV, *Plasma Physics and Controlled Fusion* **64**, 014004 (2021).
- [7] A. Marinoni, M. E. Austin, A. W. Hyatt, M. L. Walker, J. Candy, C. Chrystal, C. J. Lasnier, G. R. McKee, T. Ondříč, C. C. Petty, M. Porkolab, J. C. Rost, O. Sauter, S. P. Smith, G. M. Staebler, C. Sung, K. E. Thome, A. D. Turnbull, and L. Zeng, H-mode grade confinement in L-mode edge plasmas at negative triangularity on DIII-D, *Physics of Plasmas* **26**, 042515 (2019), <https://doi.org/10.1063/1.5091802>.
- [8] A. Balestri, P. Mantica, A. Mariani, F. Bagnato, T. Bolzonella, J. Ball, S. Coda, M. Dunne, M. Faitsch, P. Innocente, P. Muscente, O. Sauter, M. Vallar, E. Viezzer, the TCV Team, and the EUROfusion Tokamak Exploitation Team, Experiments and gyrokinetic simulations of tcv plasmas with negative triangularity in view of dtt operations, *Plasma Physics and Controlled Fusion* **66**, 065031 (2024).
- [9] T. Happel, T. Pütterich, D. Told, M. Dunne, R. Fischer, J. Hobirk, R. McDermott, U. Plank, and A. U. T. the, Overview of initial negative triangularity plasma studies on the ASDEX Upgrade tokamak, *Nuclear Fusion* **63**, 016002 (2022).
- [10] L. Aucone, P. Mantica, T. Happel, J. Hobirk, T. Pütterich, B. Vanovac, C. F. B. Zimmermann, M. Bernert, T. Bolzonella, M. Cavedon, M. Dunne, R. Fischer, P. Innocente, A. Kappatou, R. M. McDermott, A. Mariani, P. Muscente, U. Plank, F. Sciortino, G. Tardini, the EUROfusion WPTE Team, and the ASDEX Upgrade Team, Experiments and modelling of negative triangularity asdex upgrade plasmas in view of dtt scenarios, *Plasma Physics and Controlled Fusion* **66**, 075013 (2024).
- [11] A. Marinoni, S. Brunner, Y. Camenen, S. Coda, J. P. Graves, X. Lapillonne, A. Pochelon, O. Sauter, and L. Villard, The effect of plasma triangularity on turbulent transport: modeling TCV experiments by linear and non-linear gyrokinetic simulations, *Plasma Physics and Controlled Fusion* **51**, 055016 (2009).
- [12] G. Merlo, M. Fontana, S. Coda, D. Hatch, S. Janhunen, L. Porte, and F. Jenko, Turbulent transport in TCV plasmas with positive and negative triangularity, *Physics of Plasmas* **26**, 102302 (2019), <https://doi.org/10.1063/1.5115390>.
- [13] G. Merlo and F. Jenko, Interplay between magnetic shear and triangularity in ion temperature gradient and trapped electron mode dominated plasmas, *Journal of Plasma Physics* **89**, 905890104 (2023).
- [14] A. Balestri, J. Ball, S. Coda, D. J. Cruz-Zabala, M. Garcia-Munoz, and E. Viezzer, Physical insights from the aspect ratio dependence of turbulence in negative triangularity plasmas, *Plasma Physics and Controlled Fusion* **66**, 075012 (2024).
- [15] G. Di Giannatale, A. Bottino, S. Brunner, M. Murugappan, and L. Villard, System size scaling of triangularity effects on global temperature gradient-driven gyrokinetic simulations, *Plasma Physics and Controlled Fusion* (2024).
- [16] J. Ball and S. Brunner, Local gyrokinetic simulations of tokamaks with non-uniform magnetic shear, *Plasma Physics and Controlled Fusion* **65**, 014004 (2022).
- [17] A. O. Nelson, L. Schmitz, T. Cote, J. F. Parisi, S. Stewart, C. Paz-Soldan, K. E. Thome, M. E. Austin, F. Scotti, J. L. Barr, A. Hyatt, N. Leuthold, A. Marinoni, T. Neiser, T. Osborne, N. Richner, A. S. Welander, W. P. Wehner, R. Wilcox, T. M. Wilks, and J. Yang, Characterization of the elm-free negative triangularity edge on diii-d (2024), [arXiv:2405.11082](https://arxiv.org/abs/2405.11082) [physics.plasm-ph].
- [18] H.-S. Bosch and G. Hale, Improved formulas for fusion cross-sections and thermal reactivities, *Nuclear Fusion* **32**, 611 (1992).
- [19] O. Sauter, Geometric formulas for system codes including the effect of negative triangularity, *Fusion Engineering and Design* **112**, 633 (2016).
- [20] R. J. Goldston, Energy confinement scaling in tokamaks: some implications of recent experiments with ohmic and strong auxiliary heating, *Plasma Physics and Controlled Fusion* **26**, 87 (1984).
- [21] J. Rice, J. Citrin, N. Cao, P. Diamond, M. Greenwald, and B. Grierson, Understanding loc/soc phenomenology in tokamaks, *Nuclear Fusion* **60**, 105001 (2020).
- [22] G. Lamps and I. S. of Plasma Physics, *Basic Physical Processes of Toroidal Fusion Plasmas: Proceedings of* Basic Physical Processes of Toroidal Fusion Plasmas: Proceedings of the Course and Workshop Held at Villa Monastero, Varenna, Italy, August 26-September 3, 1985 No. Bd. 1 (Monotypia Franchi, 1986).
- [23] I. P. E. G. on Confinement, Transport, I. P. E. G. on Confinement Modelling, Database, and I. P. B. Ed-

- itors, Chapter 2: Plasma confinement and transport, *Nuclear Fusion* **39**, 2175 (1999).
- [24] P. Yushmanov, T. Takizuka, K. Riedel, O. Kardaun, J. Cordey, S. Kaye, and D. Post, Scalings for tokamak energy confinement, *Nuclear Fusion* **30**, 1999 (1990).
- [25] C. Paz-Soldan, C. Chrystal, P. Lunia, A. O. Nelson, K. E. Thome, M. E. Austin, T. B. Cote, A. W. Hyatt, A. Marinoni, T. H. Osborne, M. Pharr, O. Sauter, F. Scotti, T. M. Wilks, and H. S. Wilson, Simultaneous access to high normalized current, pressure, density, and temperature in a tokamak, *Nuclear Fusion* **63**, 046001 (2023), [arXiv:2309.03689](https://arxiv.org/abs/2309.03689) [physics.plasm-ph].
- [26] M. Collaboration, G. Rutherford, H. S. Wilson, A. Saltzman, D. Arnold, J. L. Ball, S. Benjamin, R. Bielajew, N. de Boucaud, M. Calvo-Carrera, R. Chandra, H. Choudhury, C. Cummings, L. Corsaro, N. DaSilva, R. Diab, A. R. Devitre, S. Ferry, S. J. Frank, C. J. Hansen, J. Jerkins, J. D. Johnson, P. Lunia, J. van de Lindt, S. Mackie, A. D. Maris, N. R. Mandell, M. A. Miller, T. Mouratidis, A. O. Nelson, M. Pharr, E. E. Peterson, P. Rodriguez-Fernandez, S. Segantini, M. Tobin, A. Velberg, A. M. Wang, M. Wigram, J. Witham, C. Paz-Soldan, and D. G. Whyte, Manta: A negative-triangularity naseem-compliant fusion pilot plant (2024), [arXiv:2405.20243](https://arxiv.org/abs/2405.20243) [physics.plasm-ph].
- [27] K. Ikeda, Progress in the iter physics basis, *Nuclear Fusion* **47**, E01 (2007).
- [28] G. Federici, C. Bachmann, L. Barucca, C. Baylard, W. Biel, L. Boccaccini, C. Bustreo, S. Ciattaglia, F. Cismonti, V. Corato, C. Day, E. Diegele, T. Franke, E. Gaio, C. Gliss, T. Haertl, A. Ibarra, J. Holden, G. Keck, R. Kentel, S. Agullo-Lopez, F. Martignol, A. Morris, B. Meszaros, I. Moscato, G. Pintsuk, M. Siccino, N. Taylor, M. Tran, C. Vorpahl, H. Walden, and J. You, Overview of the demo staged design approach in europe, *Nuclear Fusion* **59**, 066013 (2019).
- [29] M. Greenwald, Density limits in toroidal plasmas, *Plasma Physics and Controlled Fusion* **44**, R27 (2002).
- [30] F. Troyon, A. Roy, W. A. Cooper, F. Yasseen, and A. Turnbull, Beta limit in tokamaks. experimental and computational status, *Plasma Physics and Controlled Fusion* **30**, 1597 (1988).